U.S. Department of Transportation

Federal Railroad Administration

Ground Penetrating Radar Technology Evaluation and Implementation: Phase 2

Office of Research,
Development
and Technology
Washington, DC 20590

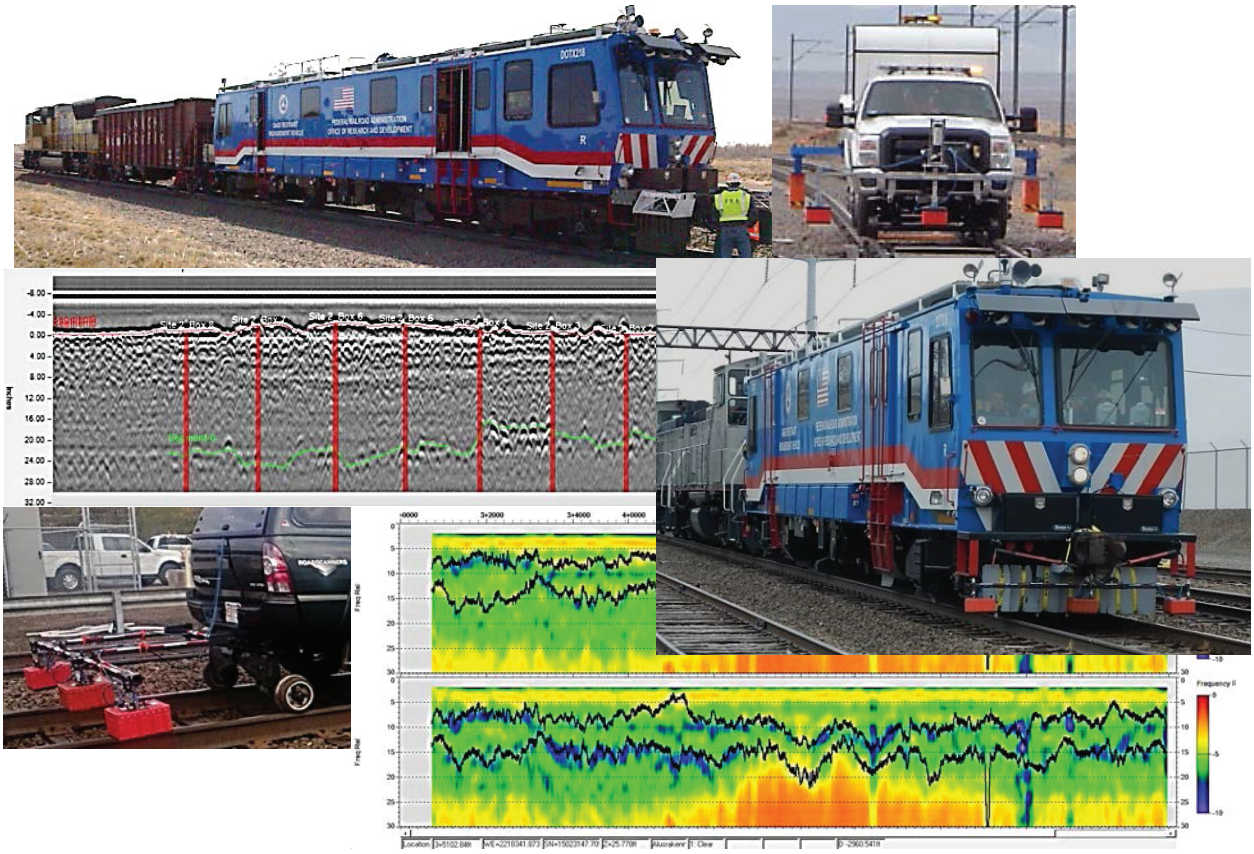

DOT/FRA/ORD-17/19

Final Report
September 28, 2017

REPORT DOCUMENTATION PAGE

Form Approved
OMB No. 0704-0188

1. AGENCY USE ONLY (Leave blank)	2. REPORT DATE	3. REPORT TYPE AND DATES COVERED
	September 28, 2017	March 2014

4. TITLE AND SUBTITLE
Ground Penetrating Radar Technology Evaluation and Implementation: Phase 2

5. FUNDING NUMBERS
DTFR53-00-C-00012
Task Order 248

6. AUTHOR(S)
Mike Brown and Dingqing Li

7. PERFORMING ORGANIZATION NAME(S) AND ADDRESS(ES)
Transportation Technology Center, Inc.
55500 DOT Road
Pueblo, CO 81001

8. PERFORMING ORGANIZATION REPORT NUMBER

9. SPONSORING/MONITORING AGENCY NAME(S) AND ADDRESS(ES)
U.S. Department of Transportation
Federal Railroad Administration
Office of Research, Development and Technology
Washington, DC 20590

10. SPONSORING/MONITORING AGENCY REPORT NUMBER
DOT/FRA/ORD-17/19

11. SUPPLEMENTARY NOTES
COR: Hugh Thompson

12a. DISTRIBUTION/AVAILABILITY STATEMENT
This document is available to the public through the FRA Web site at http://www.fra.dot.gov.

12b. DISTRIBUTION CODE

13. ABSTRACT (Maximum 200 words)

This report summarizes the results from Phase 2 of the ground penetrating radar (GPR) technologies evaluation performed by the Transportation Technology Center, Inc. at the revenue service monitoring sites on the Union Pacific Railroad and Amtrak. The scope of work included evaluation of ballast fouling and moisture sensitivity of two commercial GPR systems. An evaluation of the GPR systems installed on the DOTX 218 track inspection vehicle was also performed.

14. SUBJECT TERMS
Ground penetrating radar technology, GPR, fouling, ballast

15. NUMBER OF PAGES
39

16. PRICE CODE

17. SECURITY CLASSIFICATION OF REPORT	18. SECURITY CLASSIFICATION OF THIS PAGE	19. SECURITY CLASSIFICATION OF ABSTRACT	20. LIMITATION OF ABSTRACT
Unclassified	Unclassified	Unclassified	

NSN 7540-01-280-5500

Standard Form 298 (Rev. 2-89)
Prescribed by
ANSI Std. 239-18
298-102

METRIC/ENGLISH CONVERSION FACTORS

ENGLISH TO METRIC	METRIC TO ENGLISH
LENGTH (APPROXIMATE)	**LENGTH (APPROXIMATE)**
1 inch (in) = 2.5 centimeters (cm)	1 millimeter (mm) = 0.04 inch (in)
1 foot (ft) = 30 centimeters (cm)	1 centimeter (cm) = 0.4 inch (in)
1 yard (yd) = 0.9 meter (m)	1 meter (m) = 3.3 feet (ft)
1 mile (mi) = 1.6 kilometers (km)	1 meter (m) = 1.1 yards (yd)
	1 kilometer (km) = 0.6 mile (mi)
AREA (APPROXIMATE)	**AREA (APPROXIMATE)**
1 square inch (sq in, in^2) = 6.5 square centimeters (cm^2)	1 square centimeter (cm^2) = 0.16 square inch (sq in, in^2)
1 square foot (sq ft, ft^2) = 0.09 square meter (m^2)	1 square meter (m^2) = 1.2 square yards (sq yd, yd^2)
1 square yard (sq yd, yd^2) = 0.8 square meter (m^2)	1 square kilometer (km^2) = 0.4 square mile (sq mi, mi^2)
1 square mile (sq mi, mi^2) = 2.6 square kilometers (km^2)	10,000 square meters (m^2) = 1 hectare (ha) = 2.5 acres
1 acre = 0.4 hectare (he) = 4,000 square meters (m^2)	
MASS - WEIGHT (APPROXIMATE)	**MASS - WEIGHT (APPROXIMATE)**
1 ounce (oz) = 28 grams (gm)	1 gram (gm) = 0.036 ounce (oz)
1 pound (lb) = 0.45 kilogram (kg)	1 kilogram (kg) = 2.2 pounds (lb)
1 short ton = 2,000 pounds (lb) = 0.9 tonne (t)	1 tonne (t) = 1,000 kilograms (kg)
	= 1.1 short tons
VOLUME (APPROXIMATE)	**VOLUME (APPROXIMATE)**
1 teaspoon (tsp) = 5 milliliters (ml)	1 milliliter (ml) = 0.03 fluid ounce (fl oz)
1 tablespoon (tbsp) = 15 milliliters (ml)	1 liter (l) = 2.1 pints (pt)
1 fluid ounce (fl oz) = 30 milliliters (ml)	1 liter (l) = 1.06 quarts (qt)
1 cup (c) = 0.24 liter (l)	1 liter (l) = 0.26 gallon (gal)
1 pint (pt) = 0.47 liter (l)	
1 quart (qt) = 0.96 liter (l)	
1 gallon (gal) = 3.8 liters (l)	
1 cubic foot (cu ft, ft^3) = 0.03 cubic meter (m^3)	1 cubic meter (m^3) = 36 cubic feet (cu ft, ft^3)
1 cubic yard (cu yd, yd^3) = 0.76 cubic meter (m^3)	1 cubic meter (m^3) = 1.3 cubic yards (cu yd, yd^3)
TEMPERATURE (EXACT)	**TEMPERATURE (EXACT)**
[(x-32)(5/9)] °F = y °C	[(9/5) y + 32] °C = x °F

QUICK INCH - CENTIMETER LENGTH CONVERSION

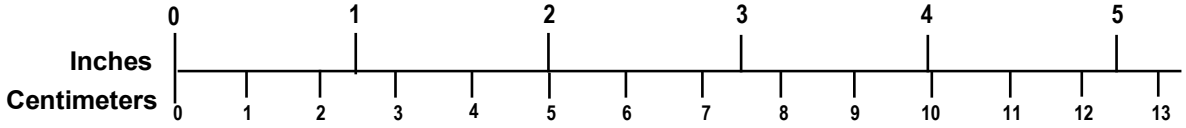

QUICK FAHRENHEIT - CELSIUS TEMPERATURE CONVERSIO

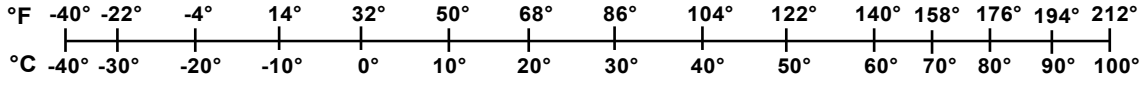

For more exact and or other conversion factors, see NIST Miscellaneous Publication 286, Units of Weights and Measures. Price $2.50 SD Catalog No. C13 10286

Updated 6/17/98

Acknowledgements

TTCI wishes to acknowledge and thank the following organizations and individuals that participated in this project:

- 3D Radar: Andy Stevens
- Amtrak: Mike Trosino and Steve Chrismer
- Balfour Beatty Infrastructure, Inc.: Steve Atherton
- Federal Railroad Administration: Hugh Thompson and Mahmood Fateh
- HyGround Engineering: Jim Hyslip, Mike LaValley, and Aaron Judge
- Roadscanners Oy: Mika Silvast and Bruce Wiljanen
- Union Pacific Railroad: Caleb Douglas and Dwight Clark
- Volpe Center: Ted Sussmann and Wesley Mui
- Zetica Rail: Asger Eriksen and Jon Gascoyn

Contents

Illustrations

Tables

Executive Summary

This report summarizes results from Phase 2 of the evaluation and implementation of ground penetrating radar (GPR) technologies performed by Transportation Technology Center, Inc. (TTCI). The work was carried out as part of Federal Railroad Administration (FRA) Task Order 248, "Ground Penetrating Radar Evaluation and Implementation." TTCI performed repeated GPR surveys at revenue service locations with two of the commercial GPR systems (systems 1 and 3) initially evaluated in Phase 1 of this study [1]. The objectives during Phase 2 were to:

- Determine the sensitivity of the GPR signal scattering method used by System 1 to ballast particle size degradation.
- Investigate the relationship between ballast moisture and fouling assessment capabilities of the dielectric dispersion analysis method used by System 3.
- Install both GPR systems on the FRA DOTX218 (T18) track inspection vehicle and compare the results with those from the standard hi-rail platform.

Two revenue service sites were established:

- The eastern site, located on Amtrak's Springfield Line, Track 1, between Milepost (MP) 3.14 (Benton Street crossing) and MP 6.37 (Stiles Lane crossing) near New Haven, CT, was established to investigate the relationship between ballast moisture and fouling interpretation using the 400-MHz antennas and dielectric dispersion fouling analysis of System 3. GPR surveys were performed by System 3 at the eastern site on September 10, 2012, April 30, 2013, and May 24, 2013. The evaluation also included results of a survey of the entire Springfield line performed on September 15, 2011, by System 3 while under contract to Amtrak.
- The western site located on the Union Pacific Railroad (UP) South Morrill subdivision, Track 2, between MP 49.0 and 51.0 near Ogallala, NE, was established to investigate the sensitivity of the 2-GHz signal and scattering analysis of System 1 to changes in ballast particle size breakdown under heavy axle load traffic. The western site also included a ballast box test installed by UP in late 2010 and supported by TTCI to monitor degradation of different ballast types. GPR surveys were carried out by System 1 at the western site in May 2012, October 2012, and March 2013.

The T18 track inspection vehicle evaluation was also performed at both sites with System 1 installed on the car for the western site survey in March 2013 and System 3 installed for the eastern site survey in late April 2013.

Results from the western site indicated that scattering analysis of the 2-GHz GPR signal provided a repeatable and stable method of determining ballast fouling that can be used to monitor changes in fouling over time. Results obtained over the 2-mile track segment (MP 49 to 51) showed no significant change in ballast fouling. The modeled fouling index (FI) varied from clean to moderately clean ballast.

GPR surveys of the eastern site by System 3 were able to discern changes in the moisture within the ballast and subballast layers, as well as at the ballast/sub-ballast/subgrade interfaces, that correlated well with localized rainfall events recorded by National Oceanic and Atmospheric

Administration (NOAA). The eastern site evaluation also confirmed the influence of moisture on the interpretation of ballast layer depth and fouling using the dielectric dispersion technique. Changes in moisture influence the layer depth calculation, which, in turn, influences the fouling analysis. Development of the frequency-relation analysis tool for moisture profile interpretation by System 3 appeared to enhance the ability to adjust the dielectric value in the fouling window analysis.

GPR systems 1 and 3 were both successfully installed on the T18 inspection vehicle. Both systems were integrated into the T18 location, track geometry, and gage restraint measuring systems (GRMS). System 3 deployed all three 400-MHz antennas in the same track positions as used with the hi-rail platform (i.e., track center and both ballast shoulders). System 1 deployed the 2-GHz antennas on the shoulders and only the 400-MHz antenna at the track center.

The outputs from both systems installed on the T18 vehicle were comparable to the hi-rail based surveys over the same track segment performed the following day. The following conclusion was confirmed: truck-mounted antennas worked much better than pilot or vehicle body mounting. Truck-mounted antennas reduced clearance issues and interference from running rails on curves. There did not appear to be significant limitations to data collection speeds for GPR technology. Modern data acquisition equipment has sufficient collection bandwidths to accommodate high speed GPR inspections.

1. Introduction

Recognizing the ongoing development of GPR as a track substructure assessment tool with the potential to produce information that contributes to track safety and performance improvements, FRA initiated Task Order 248 with the following specific goals:

- Evaluate and benchmark existing GPR techniques and capabilities.
- Provide basic recommendations and guidelines for GPR implementation.
- Investigate the viability of GPR technologies operating on FRA track inspection vehicles.
- Identify research needs for continued GPR development.

This report summarizes results from Phase 2 of the evaluation and implementation of GPR technologies performed by TTCI for FRA between March 2012 and October 2013 under this task order. Additional support for the project was provided by the Association of American Railroads (AAR) through the Improved Track Substructure Strategic Research Initiative.

1.1 Background

The development of GPR as a track substructure assessment tool has benefitted over the past 10 years from research sponsored by FRA, AAR, universities, and the internal research efforts of GPR providers. At present, GPR has the capability and is being used by some North American railroads to characterize ballast conditions over hundreds of track miles annually for maintenance planning purposes. GPR is also being used to address localized substructure issues, such as subgrade deformation and drainage problems, as well as for maintenance planning and prioritization. In either case, GPR has the capability to nondestructively visualize otherwise invisible track substructure conditions.

This research study was implemented in two phases. Phase 1 included an evaluation of six GPR systems from North America and Europe and was performed by TTCI in late 2010 at the Facility for Accelerated Service Testing on the High Tonnage Loop (HTL) in Pueblo, CO [1]. Each system was a unique combination of antenna type/frequency and methodology for ballast fouling analysis, as Table 1 describes. Systems 1, 3, and 6 were established GPR providers and the remaining systems were assembled strictly for the evaluation.

Table 1. Summary of Phase 1 GPR Systems

System	Antenna Description	Ballast Fouling Analysis
1	Pulsed radar 400 MHz for layer depth mapping and 2 GHz for ballast fouling	Radar signal scattering
2	Pulsed radar 1 GHz	Dielectric dispersion
3	Pulsed radar 400 MHz, Service Provider 1	Dielectric dispersion

4	Pulsed radar 400 MHz, Service Provider 2	Dielectric dispersion
5	Stepped frequency continuous wave radar 250 MHz—2 GHz, Service Provider 3	Dielectric dispersion
6	Pulsed radar 400 MHz and 900 MHz, Service Provider 2	Propagation analysis of the 400 MHz signal

Ballast fouling, ballast layer thickness, and moisture sensitivity outputs from each system were compared with one another and with conditions known over selected track segments. All the systems produced acceptably accurate layer thickness and moisture sensitivity results.

The ballast fouling evaluation indicated that signal scattering using 2-GHz antennas and dielectric dispersion using 400-MHz antennas gave viable results. Brief descriptions of the two fouling assessment methods are as follows:

- Air-filled void spaces between particles in clean ballast act as scatterers for the wavelengths of 2-GHz GPR signals. The scattering response diminishes as the voids are filled, providing a method of distinguishing clean from fouled ballast. Signal scattering does not rely on material dielectric properties and should therefore not be influenced by variable moisture or material types.
- Dielectric dispersion analyzes changes in dielectric properties caused by fine material and adsorbed water in the ballast. The analysis involves converting the time-domain GPR signal to a frequency-domain power spectrum. Clean ballast has a larger area under the power spectrum curve than fouled/moist ballast. Dielectric dispersion has been developed for use with 400-MHz signals that have deeper subsurface penetration capability than the higher frequency signals.

Both methods produced reasonably accurate interpretations of ballast fouling, but with potential limitations. Scattering, while not influenced by moisture or material type, is dependent on the ballast void sizes being compatible with the 2-GHz wavelength. Clean ballast with particle shapes producing small void spaces that do not act as scatters may be misinterpreted as being fouled. The use of 2-GHz antennas for fouling assessment requires the use of additional lower frequency 400-MHz antennas for inspection of substructure issues deeper than approximately 30 inches (e.g., ballast pockets and subgrade surface deformation).

Dielectric dispersion is influenced by changes in moisture and material type. Therefore, ballast layers with the same percentages of fouled material, but at different moisture contents, can potentially be misinterpreted as having different levels of fouling.

2. Phase 2 Description

Continued evaluation of GPR systems 1 and 3 from Phase 1 was carried out in Phase 2 with repeated surveys at revenue service locations. Phase 2 also included a performance evaluation of the systems installed on the FRA T18 track inspection vehicle.

Ballast condition monitoring sites were established at the following locations:

- **Eastern site:** located on Amtrak's Springfield Line, Track 1, between MP 3.14 (Benton Street crossing) and MP 6.37 (Stiles Lane crossing) near New Haven, CT. The Springfield line carries relatively low density mixed freight and passenger traffic. The eastern site was established to investigate the relationship between ballast moisture and fouling interpretation using the 400-MHz antennas and dielectric dispersion fouling analysis of System 3.
- **Western site:** located on the UP South Morrill subdivision, Track 2, between MP 49.0 and 51.0 near Ogallala, NE. The South Morrill subdivision carries high density (200- to 250-million gross tons annually) heavy axle load coal traffic. The western site was established to investigate the sensitivity of the 2-GHz signal and scattering analysis of System 1 to changes in ballast particle size breakdown under heavy axle load, high tonnage traffic. The western site also included a ballast box test installed by UP in late 2010 and supported by TTCI to monitor degradation of different ballast types.

The T18 track inspection vehicle evaluation was also performed at both sites with System 1 installed on the car in March 2013 for the western site survey and System 3 installed in late April 2013 for the eastern site survey.

3. Eastern Site Evaluation

GPR surveys were performed by System 3 on September 10, 2012, April 30, 2013, and May 24, 2013, at the eastern site. The evaluation also includes results of a survey of the entire Springfield line on September 15, 2011, performed by System 3 while under contract to Amtrak. Outputs of ballast layer thickness, moisture, and FI were produced for each survey.

System 3 was hi-rail mounted. Positioning of the three 400-MHz antennas was the same as in Phase 1 with an antenna at the track center and one 4 ft outboard of the center on both shoulders (Figure 1). The stepped frequency continuous wave antenna used by System 5 of the Phase 1 evaluation was also used to survey the eastern site on April 30, 2013.

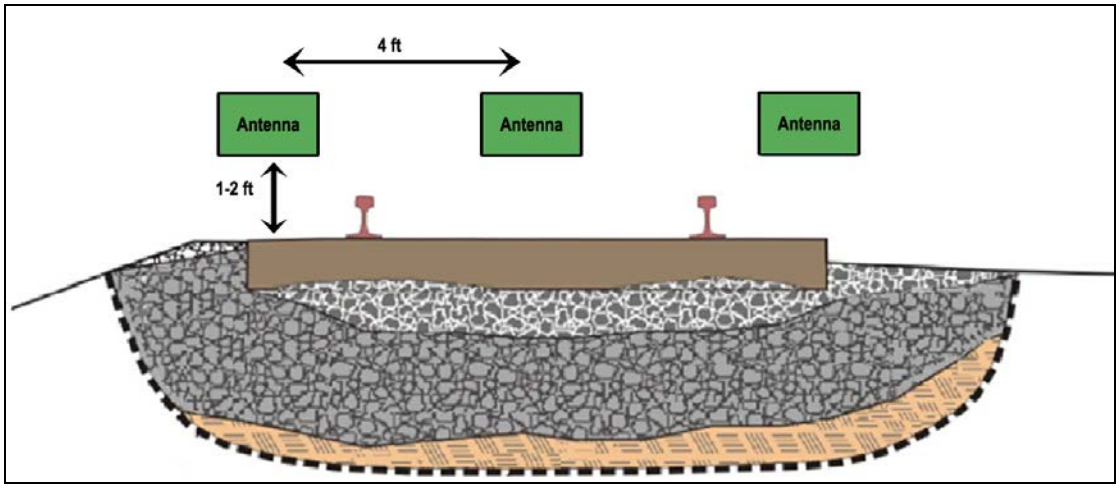

Figure 1. Positioning of System 3 400-MHz Antennas

3.1 Track Moisture Content

The focus at the eastern site was to evaluate the ability of System 3 to determine changes in track substructure moisture and to differentiate moisture conditions from ballast fouling and layer thickness conditions. Changes in the degree of ballast fouling and layer thickness over the course of the evaluation were considered negligible given the track's relatively low applied tonnage exposure. Therefore, the key variable was changing moisture levels.

Figures 2 through 5 show the precipitation history for the eastern site based on data from NOAA for New Haven, CT. Figure 2 shows the daily moisture totals between September 2011 and the end of May 2013 with the time of each GPR survey indicated. Figures 3 and 4 give the daily precipitation data 7 to 14 days prior to each survey, and Figure 5 shows the hourly rainfall amounts for the 12-hour period before the GPR surveys of September 10, 2012, and May 24, 2013.

The surveys of September 15, 2011, and April 30, 2013, were performed at least 6 days following any precipitation at the site. The survey of September 10, 2012, was performed within 8 hours of a 0.25-inch rainfall event, and the May 24, 2013, survey was the wettest, taking place approximately 10-hours after a significant rainfall event totaling nearly 1 inch.

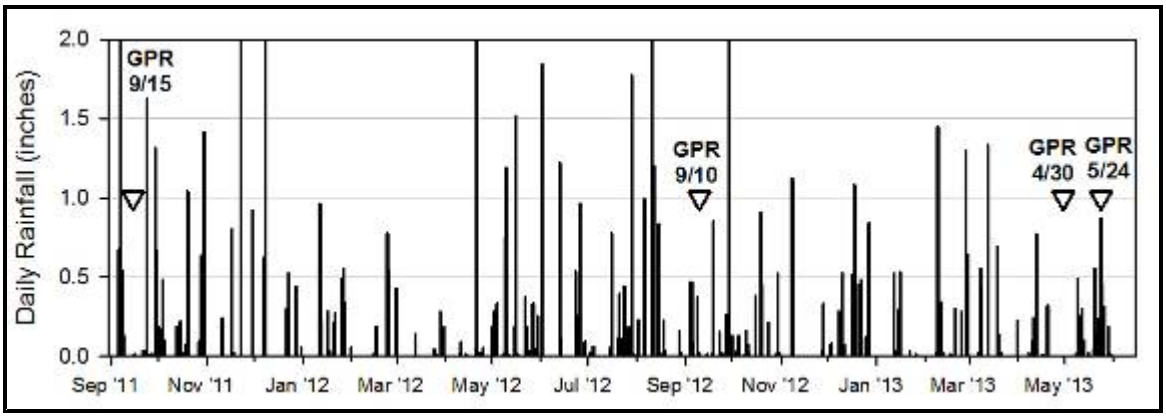

Figure 2. Daily Rainfall Amounts from NOAA Weather Station Near East GPR Test Site from September 2011 to June 2013 [1]

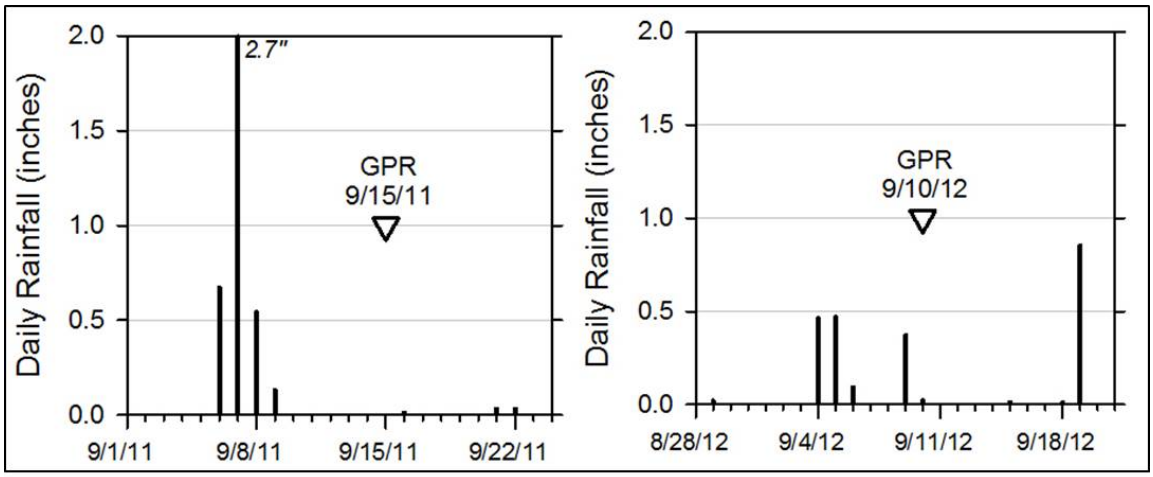

Figure 3. Daily Rainfall Amounts for September 2011 (left) and September 2012 (right)

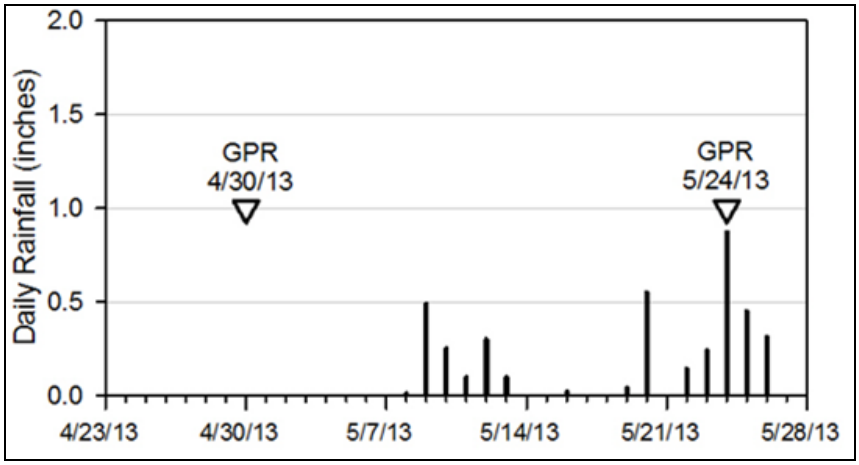

Figure 4. Daily Rainfall Amounts for April and May 2013

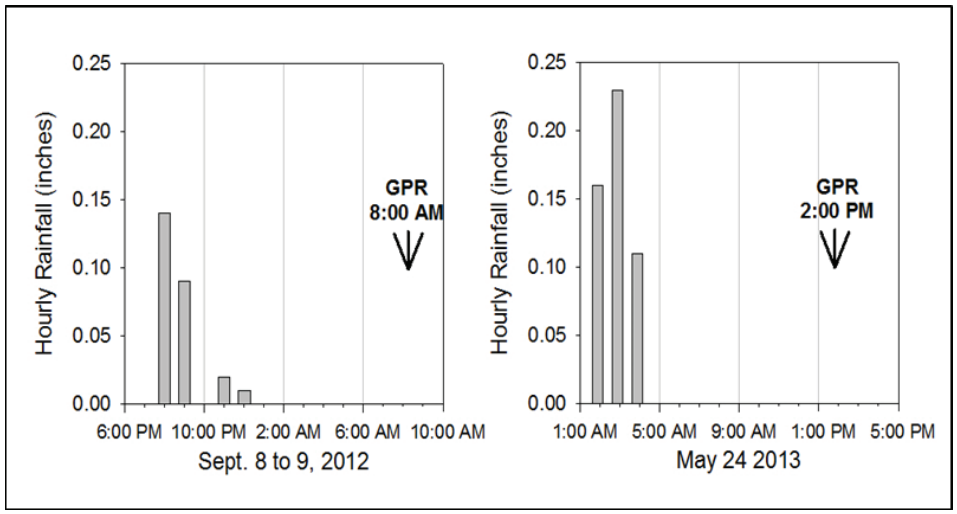

Figure 5. Hourly Rainfall Totals Prior to the September 10, 2012, and May 24, 2013, Surveys

Moisture from the eastern site surveys was visualized and investigated by analyzing the frequency response of the GPR signal. As described earlier, fine materials and increased water content affect the frequency spectrum of the received GPR information. Time-domain GPR data is transformed to the frequency-domain and parameterized by means of a sliding calculation window in the vertical (depth) and longitudinal directions. Use of a windowed Fourier frequency transformation analysis enables calculation of the frequency response at variable depths. The analysis produces moisture profiles in which the GPR data is visualized as a color-coded contour map. The increased strength of the reflected signal is caused by an increase in the moisture content and percentage of fine materials in the substructure. Weaker reflections indicate dryer materials.

As an example, Figure 6 shows the change in moisture measured by System 3 from water being added to the track center and draining laterally to the right ballast shoulder. The data in Figure 6 was taken during the Phase 1 evaluation and shows the increase in moisture after adding water to the track in the test section at Transportation Technology Center (TTC) in November 2010.

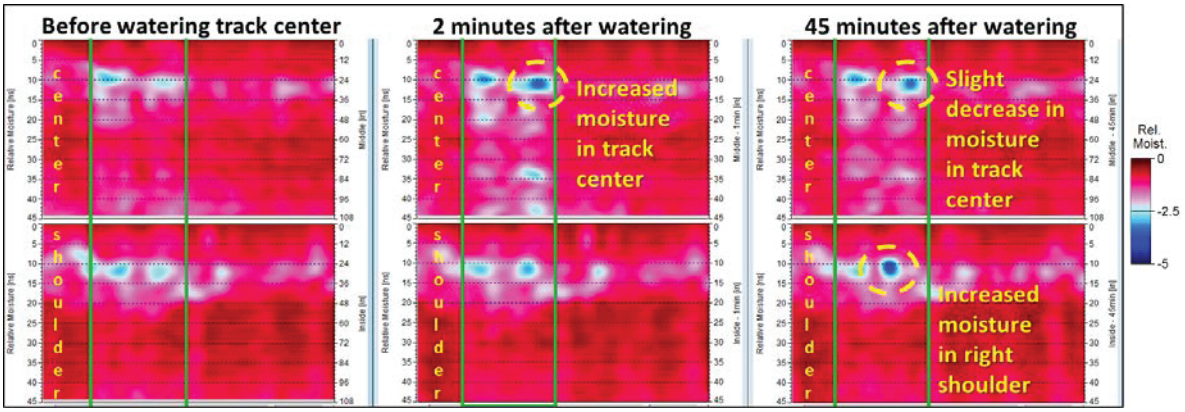

Figure 6. Example of System 3 Sensitivity to Moisture Being Added to the Track Center and Draining to Right Shoulder

Moisture profiles were calculated by System 3 using a recently developed frequency-relation analysis tool that is based on comparisons of different frequency bands in the returning GPR signal. Increasing moisture content is seen as the lower frequencies increasing against higher frequencies and is visualized in Figure 7 as increasing amounts of blue and/or violet in the profile.

Figure 7 compares the layer thickness interpretation and frequency-relation moisture profiles of the eastern site during the April 30, 2013, survey performed after several days without rain (dry track) and the May 24, 2013, survey performed 10 hours after a 1-inch rainfall (wet track). The layer thickness interpretation is similar for both surveys, as would be expected. The moisture profile, however, shows an increase in the blue-colored lower frequencies at the ballast-sub-ballast and sub-ballast-subgrade interfaces during the May 24 survey, indicating an increase in the moisture content.

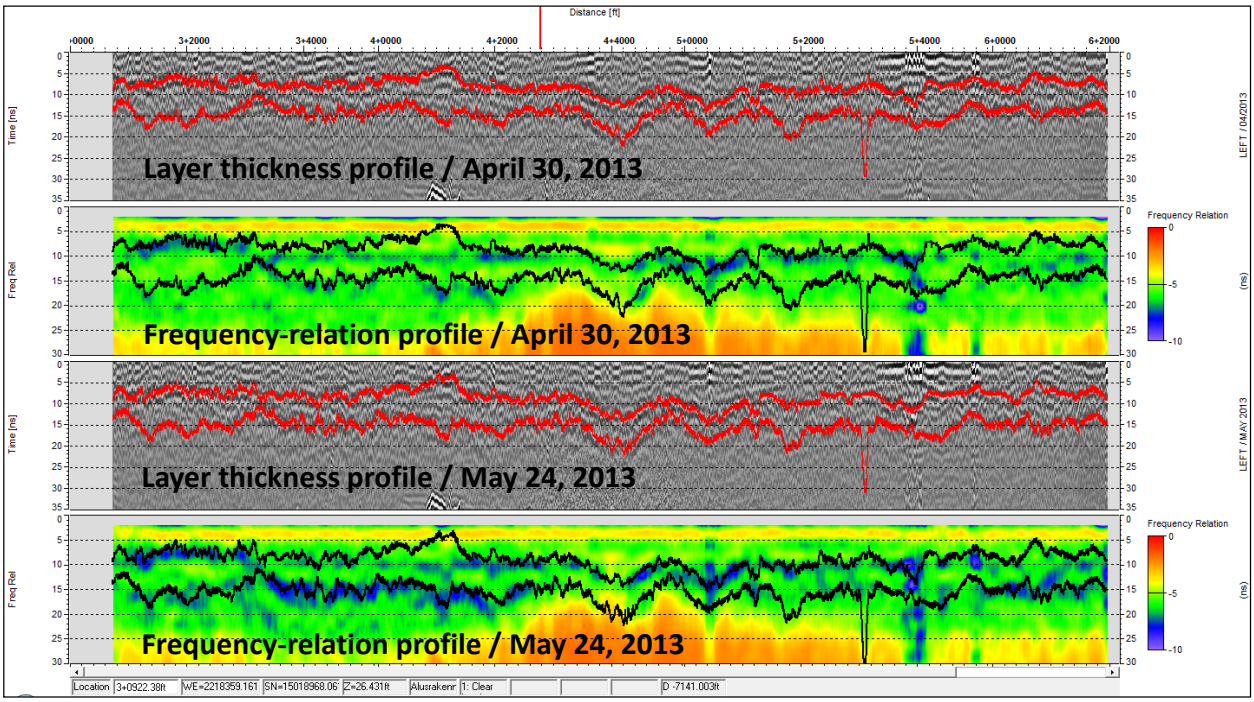

Figure 7. Frequency-Relation Moisture Profiles from the April 30, 2013, (dry track) and May 24, 2013, (wet track) Eastern Site Surveys

Figure 8 focuses on roughly the first 1.5 miles of the moisture profile data shown in Figure 7 and highlights two moisture conditions. The April 30 dry track survey indicated that some moisture was being retained at the bottom of the ballast-top of the sub-ballast interface in the first 2,400 feet of the site, but there was relatively little moisture retention at the bottom of the sub-ballast-top of the subgrade interface over the 1.5 miles. The May 24 wet track survey showed some increase in moisture at both the ballast-sub-ballast and sub-ballast-subgrade interfaces in the first 2,400 feet, but a noticeable increase in moisture at the sub-ballast-top of subgrade interface over the next mile—and little change in moisture at the top of the subballast in this zone.

Results shown in Figure 8 imply a well-drained ballast layer throughout the site, a slower draining subballast layer in the first 2,400 feet of the site, and a well-drained subballast layer in

the next mile where most of the moisture is being retained at the bottom of the subballast and top of the subgrade layer.

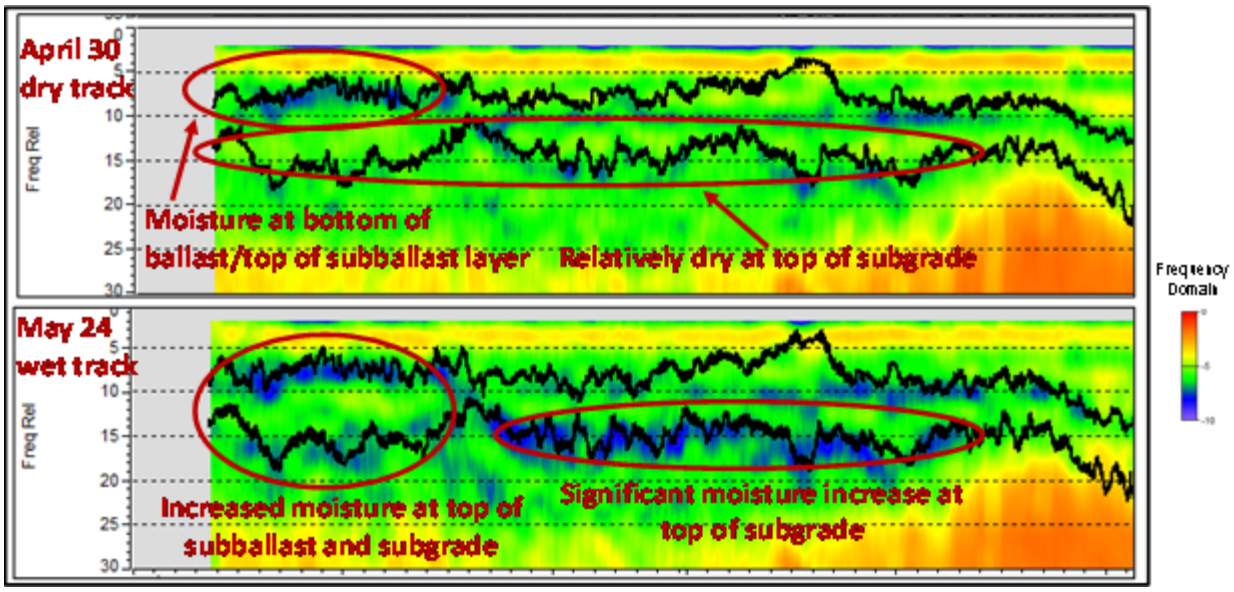

Figure 8. Comparison of GPR Moisture Interpretation at Track Substructure Layer Interfaces During the April 30 and May 24 Surveys

In addition to the frequency-relation analysis for determination of moisture presence, higher moisture content can also be assumed when longer travel times (slower velocity) of the GPR signal are detected between the bottoms of ballast and subballast layers in successive surveys. Increased moisture causes an increase in the dielectric permittivity of the material, resulting in reduced signal velocity. A slightly longer travel time through the subballast was noted during the May 24 wet track survey and was compensated for in the interpretation phase by increasing the dielectric value by one unit in locations where required.

3.2 Moisture Influence on Ballast Fouling Assessment

Slower signal velocities from increased moisture can also affect the ballast fouling interpretation when a constant signal return time window is used in the analysis. The ballast depth over which fouling is calculated is determined from the measured return time of the signal and the assumed dielectric permittivity of the material. A constant return time window will give different fouling calculation depths for different moisture conditions. Therefore, the assumed dielectric value should be adjusted to compensate for moisture changes.

Figure 9 shows the ballast fouling index (BFI) output of System 3 for all eastern site surveys (left channel) plotted against distance. The FI is the same as the Selig fouling index [2] and represents the percentage of material that is smaller than 0.187 inch (No. 4 sieve) plus the percentage smaller than 0.003 inch (No. 200 sieve). The top plot in Figure 9 shows the fouling values calculated using a constant return time window. As pointed out earlier, the researchers assumed that the fouling at the site would not change over the course of the evaluation. However, the May 24 wet track survey shows slightly lower fouling values in some locations in the constant return

time window plot; this change in values resulted from moisture which caused slower travel time and shallower calculation depths. The bottom plot is the same data, but fouling is calculated using an interpreted ballast bottom for reference depth. The same results in the bottom plot could be achieved by using a deeper constant depth time window for moist ballast. The results in Figure 9 show that moisture is causing relatively small differences in the fouling output.

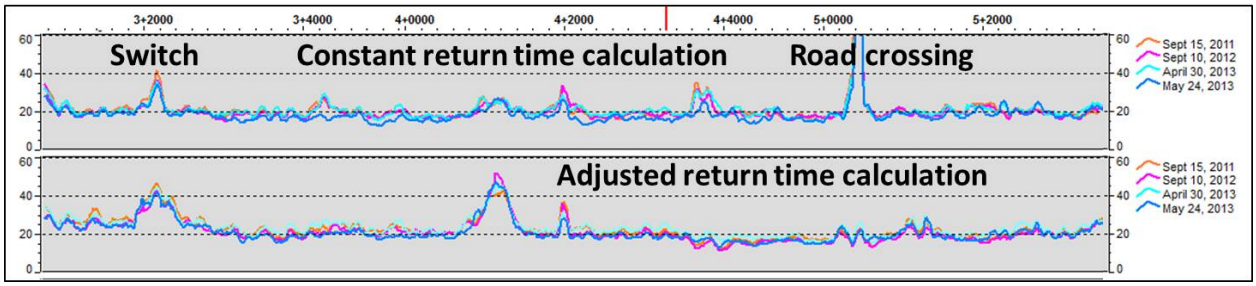

Figure 9. Eastern Site Ballast Fouling Results

4. Western Site Evaluation

GPR surveys were carried out by System 1 at the western site in May 2012, October 2012, and March 2013. The GPR surveys were performed on the UP South Morrill subdivision, Track 2, between MP 49.0 and MP 51.0. The survey limits encompassed the UP ballast box test zones located at MP 50.50 (curve track) and MP 50.05 (tangent track). In addition to the 2-mile data collection runs, data was acquired at higher resolution (12 scans per foot compared with the normal 4 scans per foot) over the shorter track segments encompassing the ballast box zones. The high-resolution data was used for detailed analysis of ballast fouling in the boxes.

System 1 was hi-rail mounted, with the antennas positioned at the track center and both shoulders (Figure 10). Data was acquired using a SIR-30 GPR control unit. The antenna configuration included:

- Three 2-GHz horn antennas used primarily for ballast fouling analysis to a depth of 30 inches; and
- Three 400-MHz bow-tie antennas used for substructure interfaces to a depth of approximately 60 inches.

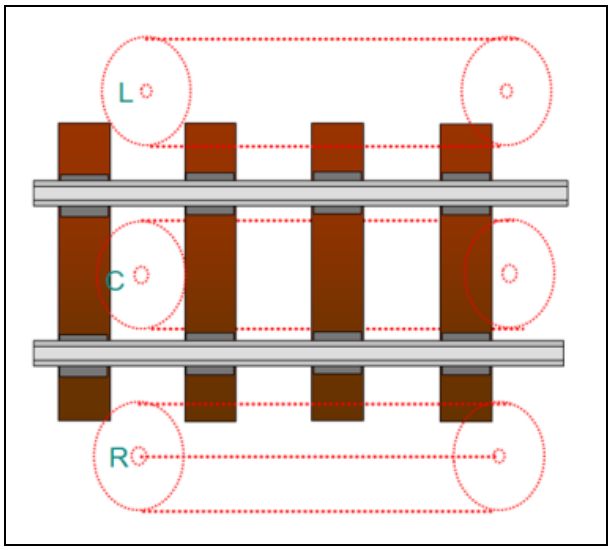

Figure 10. Position of System 1 Antennas and Antenna Footprints

4.1 Ballast Fouling Assessment

As described earlier, ballast fouling was determined by System 1 through analysis of the 2-GHz scattering response within the ballast layer. The two-dimensional (2D) scattering response was visualized as a colored map, as shown in Figure 11, with red indicating relatively fouled ballast and yellow-green signaling relatively clean ballast. The 2D map provides a visual indication of the distribution of fouling within the ballast layer.

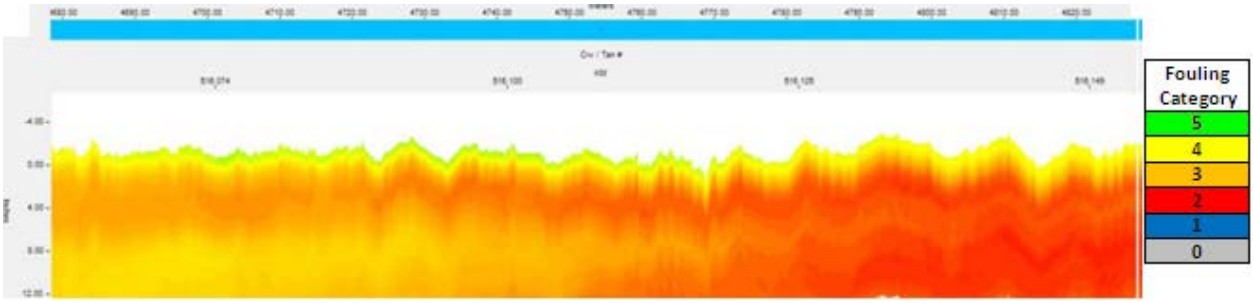

Figure 11. System 1 2D Ballast Fouling Representation

In addition to the 2D map, fouling results were also presented in the form of one-dimensional (1D) fouling values. The 1D BFI was the approximate equivalent of Selig's fouling index [2], representing the average of the 2D map from the surface to a depth of 16–18 inches over a distance of 6 feet along the track. The BFI was divided into relative fouling categories ranging from clean (BFI < 5%), moderately clean (BFI 5%–10%), moderately fouled (BFI 10%–25%), fouled (BFI 25%–30%), and severely fouled (BFI > 30%). An additional category 0 was used where the fouling could not be analyzed because of interference from external sources of electromagnetic interference or where surface structures, such as switches or bridges, affected the GPR signal.

System 1's ballast fouling analysis capabilities were enhanced over the course of Phase 2. An updated antenna matching method was introduced in the summer of 2012, followed by changes to the BFI software algorithm. Results from the new algorithm were calibrated to Selig's fouling index[2] based on the May 2012 ballast gradation results.

4.1.1 Fouling Assessment MP 49–MP 51

BFI data generated by the three GPR surveys over the western site are plotted against distance in Figure 12. This plot also shows the locations and BFI from gradation analysis of five ballast samples acquired during the May 2012 survey.

The survey comparison in Figure 12 indicates reasonable agreement in the BFI output of the three data sets, as well as from the locations of isolated spikes in the level of ballast fouling. Correlation between the May 2012 ballast gradation results and the BFI analyzed, or modeled, in the May 2012 GPR survey (Table 2) is also considered reasonable.

Detailed analysis of the three data sets suggests that there had been insignificant measurable change in ballast fouling along the 2-mile section of track in the 10 months between May 2012 and March 2013. Measurable change is currently defined by System 1 as a difference of ±0.2 BFI based on antenna calibration tests carried out at System 1's test site and routine onsite calibrations.

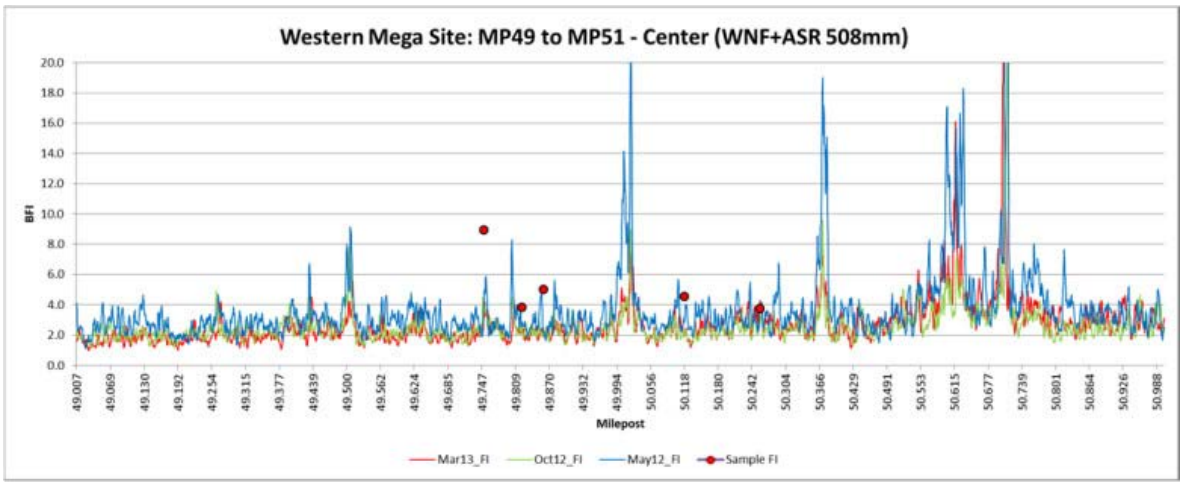

Figure 12. Track Center GPR BFI Distance History Overlay Data from Western Site Surveys

Table 2. Comparison of Track Center Western Site Sample and GPR BFIs from May 2012 Survey

Sample No.	Mile Post	Percent Passing Sieve		Sample BFI	GPR BFI
		0.375 in	0.187 in		
2	49.75	10.72	7.96	9	3
5	49.81	4.04	2.86	4	3
8	49.85	5.69	4.03	5	3
11	50.11	4.25	3.54	5	3
14	50.25	3.97	2.77	4	3

4.2 UP Ballast Box Test Assessment

A ballast test was initiated in 2010 as a joint UP and TTCI effort to monitor degradation of different ballast types in a high tonnage, heavy axle load environment. Test zones were established on tangent track at MP 50.05 and on a 2-degree curve at MP 50.50 of the UP South Morrill subdivision. Both zones included eight steel boxes that were used to separate the various ballast types (Figure 13). The boxes in the curve zone had steel bottoms and the boxes in the tangent zone had fabric bottoms. Ballast samples have been taken two times a year from the boxes installed in November 2010 for gradation analysis to monitor particle size breakdown.

The western GPR site (MP 49.0 to 51.0) overlapped the ballast box test zones, and ballast box sampling coincided with all the GPR surveys.

Figure 13. Installation of the UP Ballast Box Test

4.2.1 Curve Zone Fouling Assessment

Figure 14 is an example of processed GPR track center data acquired during the May 2013 survey over the eight ballast boxes in the curve zone. The high amplitude reflection from the steel bottoms of the boxes is identifiable, as indicated by the green line. The sides of the boxes are also identifiable and shown as the red lines.

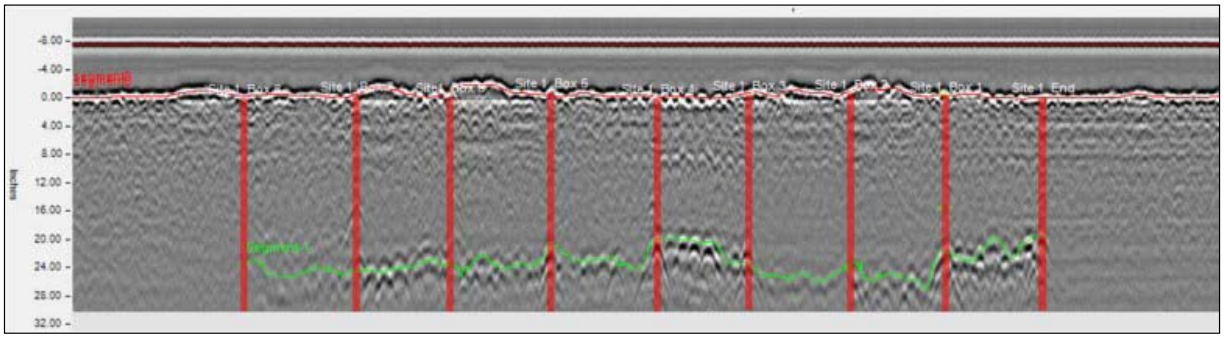

Figure 14. Processed GPR Data from the Ballast Box Test Curve Zone

Table 3 shows the BFI results for each GPR survey analyzed, or modeled, from the GPR data, along with the calculated change in BFI over each intervening period based on ballast sample sieve analysis. The differences over each period are also presented in Figure 15.

Table 3. Ballast Box Test Curve Zone BFI Results, Center Antenna

Box/Section	GPR Modeled Ballast Fouling Index			Sampled Ballast BFI Difference from Sieve Analysis		
	May 12	October 12	March 13	May 2012 to October 2012	October 2012 to March 2012	May 2012 to March 2013
8	2.0	2.6	5.6	0.6	3.0	3.6
7	1.8	2.7	6.4	0.9	3.7	4.6
6	1.9	4.0	4.2	2.1	0.2	2.3
5	4.6	3.9	4.6	-0.6	0.7	0.0
4	4.7	8.4	7.3	3.7	-1.1	2.6
3	5.1	3.3	6.9	-1.8	3.6	1.8
2	4.4	2.2	2.6	-2.2	0.5	-1.8
1	6.5	4.0	7.2	-2.4	3.2	0.7
75 ft east	0.9	2.2	2.4	1.3	0.2	1.5
75 ft west	1.0	2.6	2.4	1.6	-0.2	1.4

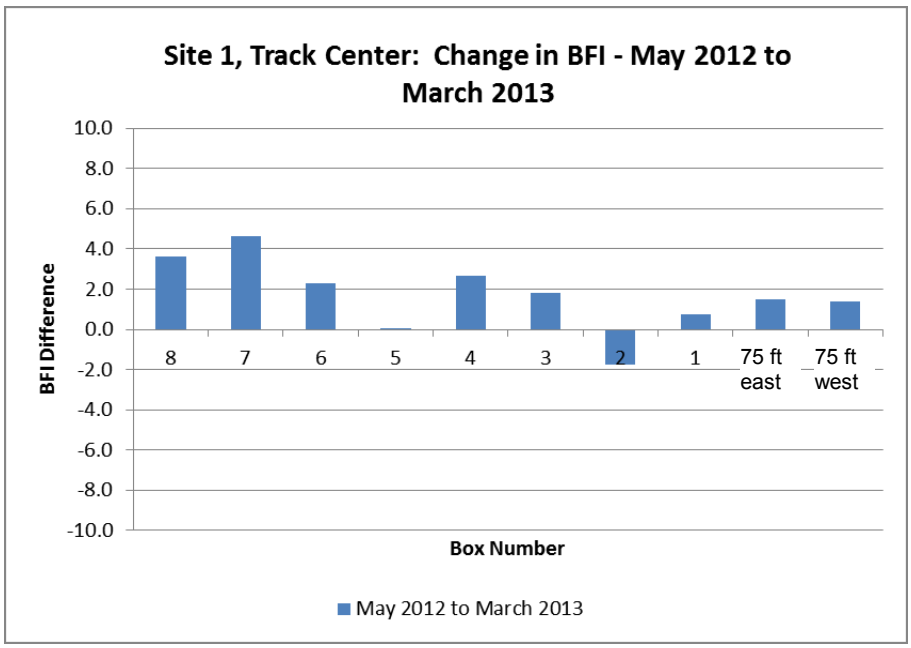

Figure 15. Ballast Box Test Curve Zone Change in BFI Over the GPR Evaluation Period

The GPR data indicates that between May 2012 and March 2013 there was either no change or a slight increase in the level of fouling. The largest difference was observed within boxes 5 to 8 which contained the control ballast for the test. The majority of the increase occurred between the October 2012 and March 2013 test dates. All the observed increases, except for those in boxes 1 and 3, exceed the 0.2 detection threshold described in subsection 4.1.1.

The nominal increase in BFI between October and March is evident in the color plots of the modeled 2D BFI presented in Figure 16. As described earlier, the 2D BFI provides a visual representation of fouling within the ballast layer, and areas of elevated fouling are identified by hotter colors (oranges and reds). The increase in fouling is identifiable in Figure 16 towards the bottom of the March 2013 2D BFI color map. The boundaries between the ballast boxes are identified by the vertical red lines.

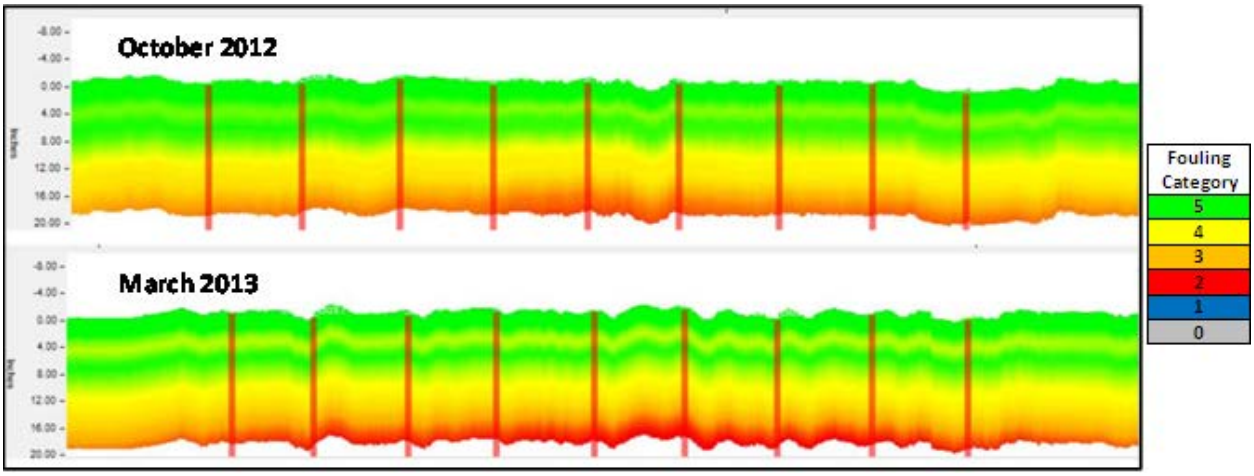

Figure 16. System 1 2D BFI Visualization for the Ballast Box Curve Zone Showing Increased Fouling at the Bottom of the Ballast Layer During the March 2013 Survey

4.2.2 Tangent Zone Fouling Assessment

Table 4 shows the modeled BFI results from the tangent ballast box test zone. A comparison of the results in the curve zone reveals a similar pattern of clean and fouled ballast in the eight boxes, with the highest levels of fouling in March 2013 evident within boxes 1 to 3. A comparison of the BFI results from the three collection dates reveals no measurable change in ballast fouling over the 10-month period, with the exception of boxes 1 and 2, which both show a nominal increase in fouling (Figure 17). The 2D BFI color maps in Figure 18 show the increased fouling towards the bottom of the March 2013 image, as observed in the curve zone.

Table 4. Ballast Box Test Tangent Zone BFI Results, Center Antenna

Box/Section	Modeled Ballast Fouling Index			BFI Difference		
	May 12	October 12	March 13	May 2012 to October 2012	October 2012 to March 2012	May 2012 to March 2013
8	2.9	3.5	4.0	0.6	0.5	1.1
7	4.0	3.9	4.9	0.0	1.0	0.9
6	1.8	3.6	3.6	1.8	-0.1	1.7
5	2.2	4.0	4.2	1.8	0.2	1.9
4	1.6	3.1	2.5	1.5	-0.6	0.9
3	7.9	6.8	7.5	-1.1	0.7	-0.3
2	3.7	10.4	9.9	6.7	-0.4	6.3
1	1.6	4.1	6.0	2.5	1.9	4.3
75 ft east	1.2	2.7	3.0	1.5	0.3	1.8
75 ft west	1.4	3.5	3.8	2.1	0.3	2.4

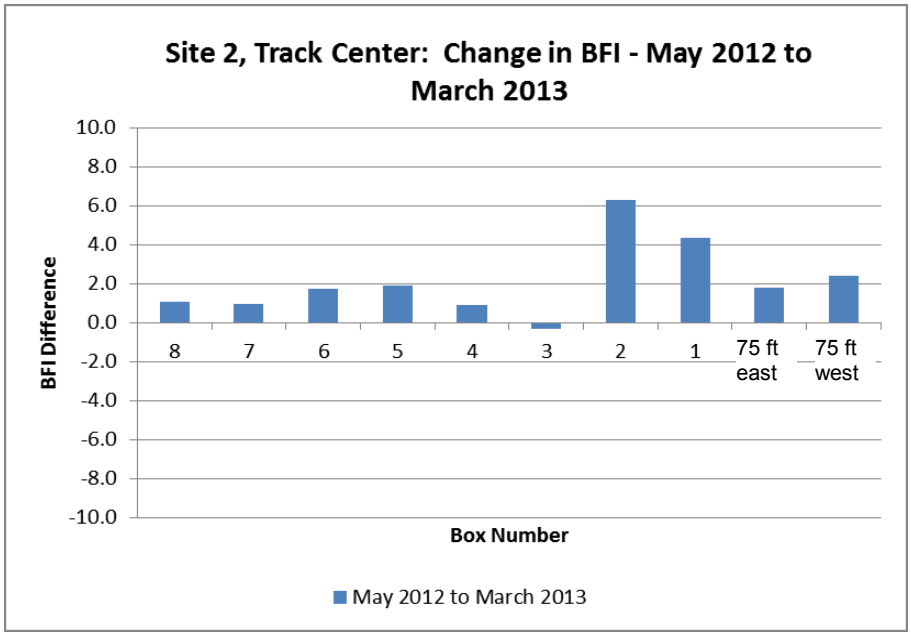

Figure 17. Ballast Box Test Tangent Zone Change in BFI Over the GPR Evaluation Period

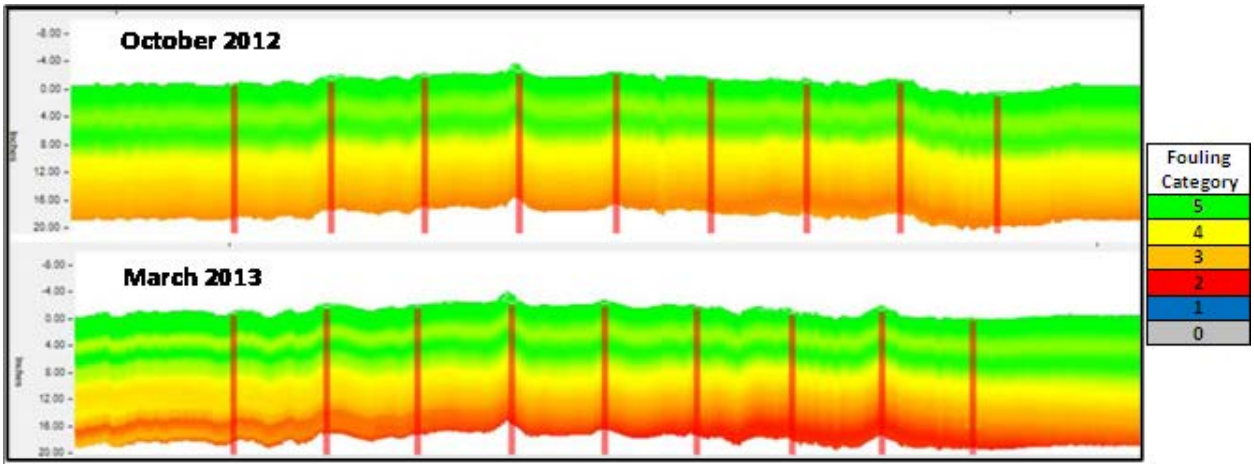

Figure 18. System 1 2D BFI Visualization for the Ballast Box Tangent Zone Showing Increased Fouling at the Bottom of the Ballast Layer During the March 2013 Survey

5. T18 Mounted GPR Technology Evaluation

The scope of Phase 2 also included evaluating GPR systems 1 and 3 installed on the T18 track inspection vehicle and surveying their respective ballast monitoring sites. The evaluation was performed to determine if the T18, or a similar rail-bound vehicle, could provide a platform for GPR data acquisition comparable to that of the standard hi-rail platform.

The System 1 survey of the western site was performed on March 20, 2013, and System 3 surveyed the eastern site on April 29, 2013. The hi-rail surveys of the sites were performed within a day of the T18 survey.

Note that the data and results submitted in Sections 3 and 4 of this report were generated by the applicable GPR system operating from a hi-rail platform in accordance with the normal antenna configuration. The data and results in Section 5 were generated by the systems installed on the T18 for the first time.

5.1 System 1 T18 Evaluation

System 1 was initially installed on the T18 vehicle at TTC on March 8, 2013. Shakedown and comparative surveys of the HTL were performed with the system installed on the T18 and hi-rail vehicles over the next 6 days.

Figure 19 shows the GPR antenna configuration installed on the T18 vehicle for System 1. The 2-GHz antennas were mounted inboard of their normal position on the hi-rail vehicle, with the center of each antenna located approximately 6 inches from the ends of the ties—in contrast to 10 inches on the hi-rail. The height of the antennas above rail was equivalent to that of the hi-rail installation. Note that the track center 2-GHz antenna normally used for ballast fouling analysis on the hi-rail vehicle was not installed on the T18 vehicle because of clearance issues.

Antennas were mounted on the rear of the T18 vehicle using custom-designed brackets, as Figure 20 shows. The T18 antenna deployment included shielded housings to minimize potential interference from stray signal reflections bouncing off the vehicle body and to reduce the effects of electromagnetic interference from external sources such as cell phone transmitters. Acquisition of the GPR data was controlled by the same SIR-30 GPR control unit used on the hi-rail.

As Figure 19 shows, the T18 GPR survey speed over the western site was 50 mph and the hi-rail speed was 20 mph.

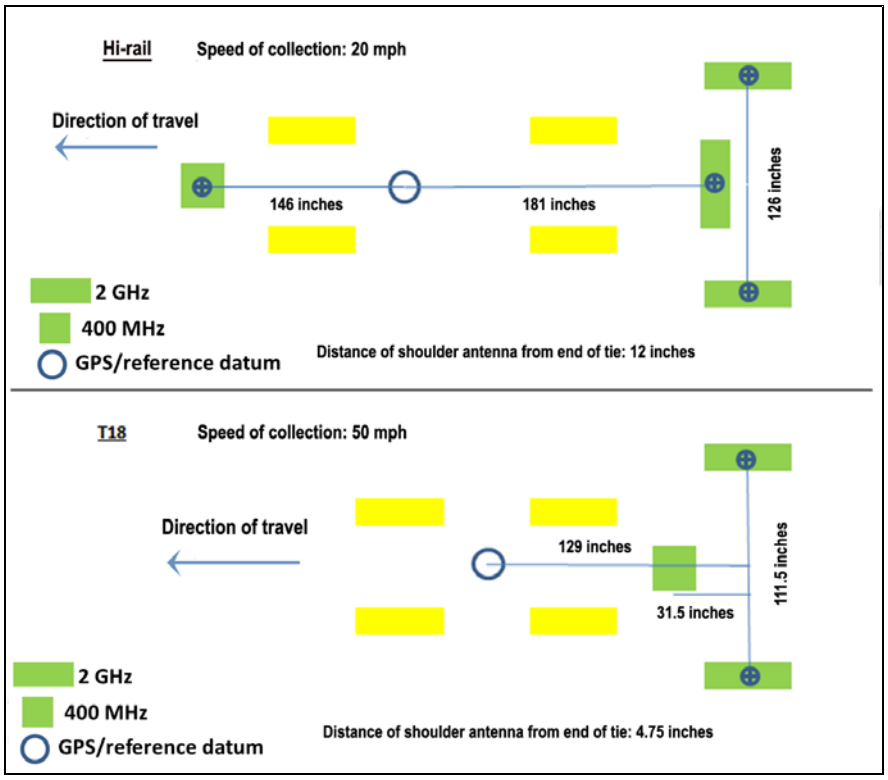

Figure 19. System 1 Hi-Rail and T18 Antenna Configuration

Figure 20. Antenna Deployment and Shielded Housings on the Rear of the T18 Vehicle

5.1.1 Fouling Comparison

Figure 21 shows a comparison of the BFI outputs (BFI data plotted against distance) for both ballast shoulders from the T18 and hi-rail surveys on March 20, 2013, at the western site. The left shoulder comparison at the top of Figure 21 indicates good agreement between the T18 and hi-rail platforms, with both surveys showing similar localized features and fouling levels almost exclusively below 5 BFI. The right shoulder data at the bottom of Figure 21 for T18 shows a slightly more fouled response than the hi-rail survey data. This response is more pronounced at areas of increased fouling level, and was thought to have been caused by the shoulder antennas being closer to the rails on the T18 compared with the hi-rail location (see Figure 19). Fouling is typically higher within the center of the track and around the rail seats than it is further out on the shoulders.

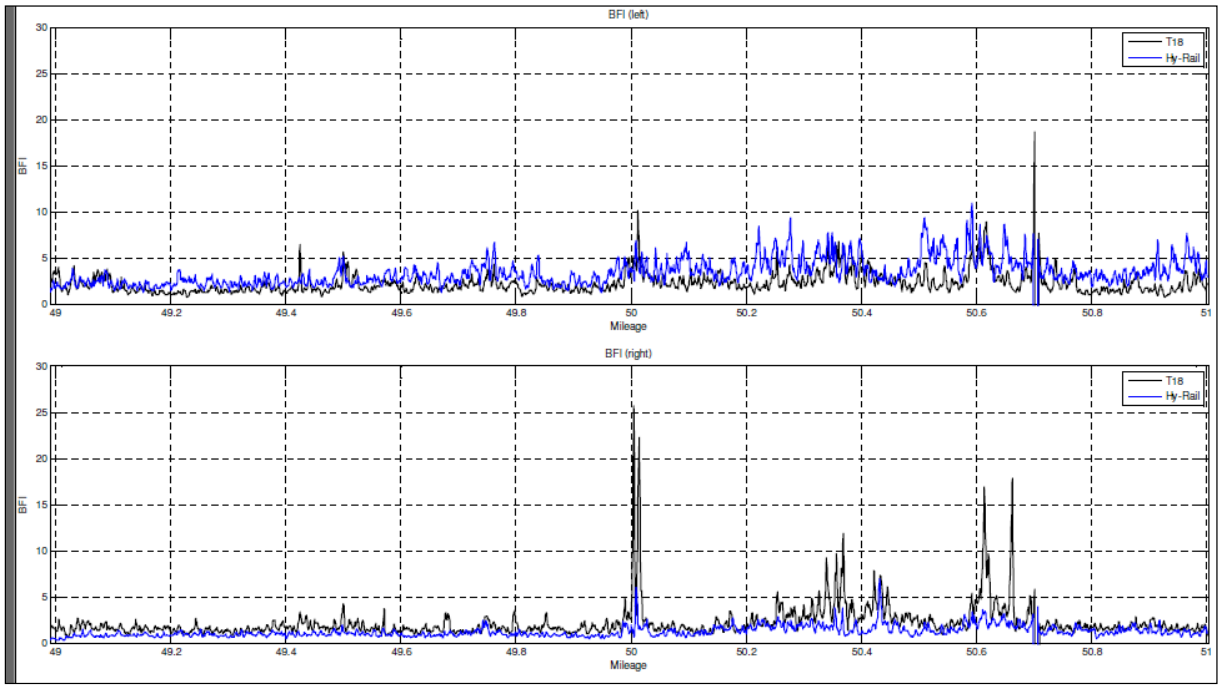

Figure 21. Ballast Shoulder Fouling Results Comparing T18 and Hi-Rail Mounted Outputs

5.1.2 Primary Layer Depth Comparison

The T18 and hi-rail primary layer depths that represent the boundary between the ballast and subballast layers were in close agreement. Both surveys produced repeatable results showing similar localized features, as well as identifying the same regional trends in the primary interface depth. Figure 22 shows the comparison of the 400-MHz track center primary layer depth outputs.

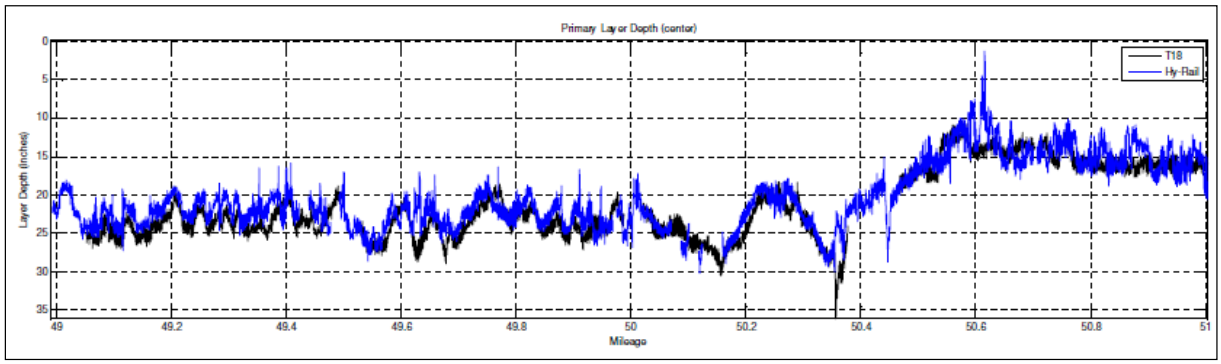

Figure 22. Comparison of Primary Layer Depth Outputs from the T18 and Hi-Rail Vehicles

5.1.3 T18 Speed Comparison

A comparison of T18 mounted System 1 results at survey speeds of 20 and 40 mph over the HTL indicated little difference in the data sets. An example is shown in Figure 23 where the HTL left shoulder FI results at 20 mph overlay the results from the 40-mph survey.

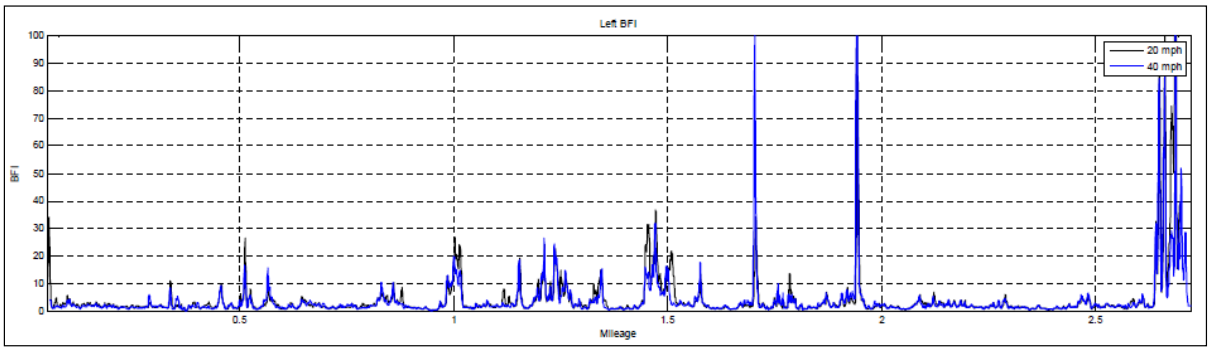

Figure 23. Left Shoulder Fouling Index Comparison of the HTL at T18 Survey Speeds of 20 and 40 mph

5.2 System 3 T18 Evaluation

The installation of the GPR System 3 antenna on the T18 vehicle closely resembled the hi-rail antenna deployment. Three 400-MHz antennas were mounted at the T18 rear platform, 12 to 14 inches above top of tie at the track center and each end of tie (Figure 24). Echo-absorbing foam was installed to minimize ringing of the radar signal from nearby metal under the T18. Two GSSI SIR-20 control units (each 2 channels) and a single SIR-30 (4 channels) control unit were used during the evaluation.

Shakedown testing of the system to ensure functionality took place at a federal facility on April 11, 2013, prior to the April 29, 2013, survey of the eastern site.

Figure 24. System 3 Installation on Rear of T18 Vehicle Showing Antennas at Track Center and Shoulders and Foam Barrier

A T18 mounted GPR survey was performed over the eastern site between MP 3.14 (Benton Street crossing) and MP 6.37 (Stiles Lane crossing) between 20 and 30 mph on April 29, 2013. A second T18 survey was performed over the Springfield line from Benton Street crossing (MP 3.14) to Springfield Station (MP 62) at speeds up to 50 mph using the SIR-30 based system.

5.2.1 Eastern Site Survey Results

On June 11, 2013, a Microsoft® Excel file of results was transmitted by System 3 to ENSCO, Inc. The Excel file contained the following data for both SIR-20 and SIR-30 controllers and for left, center, and right channels:

- Ballast thickness
- Subgrade depths
- Degree of ballast fouling (9 inches to 16 inches from top-of-tie)
- Moisture condition (9 inches to 24 inches from top-of-tie)

These data were aligned with the foot-by-foot track geometry and GRMS data from the other measurement systems on DOTX 218.

The T18 survey results were similar to the hi-rail based survey results of April 30, 2013. Figure 25 compares the left channel grayscale images with digitized layer boundaries and the ballast fouling results in plain view for both T18 and hi-rail platforms.

The slight differences between the T18 and hi-rail based fouling results were attributed to slight noise in the T18 data from the T18. In addition, there were also slight differences in fouling results from the SIR-20 and SIR-30 controllers on the T18 caused by inherent differences between the two units. The fouling results were based on calibrations with the SIR-20 based

system. Minor calibration adjustments to the SIR-30 data would produce similar fouling results as the SIR-20 data.

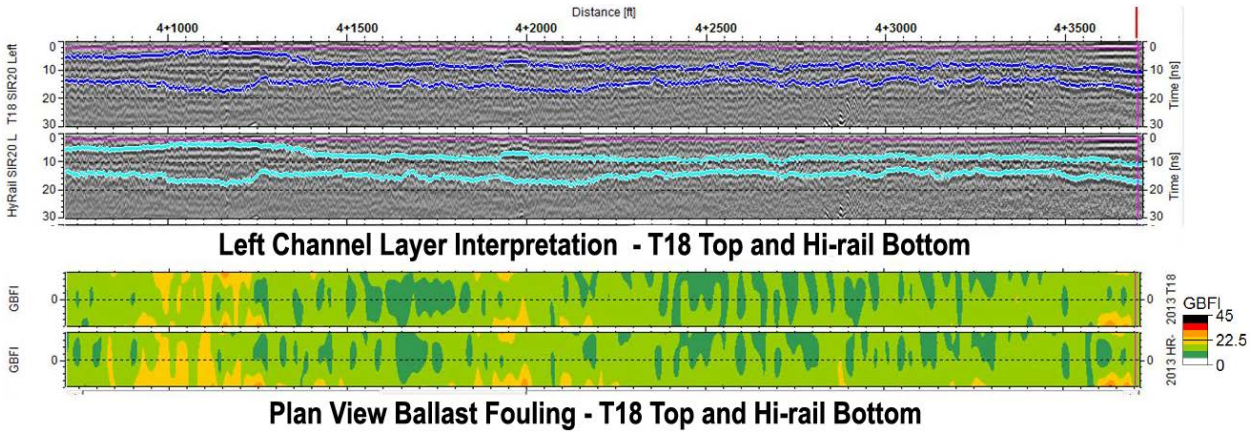

Figure 25. Comparison of System 3 T18 and Hi-Rail GPR Outputs

6. General Findings

The objective of Phase 2 was to continue investigating the track substructure assessment capabilities of GPR systems 1 and 3 from Phase 1. Specific project objectives were:

- Determine the sensitivity of the GPR signal scattering method used by System 1 to ballast particle size degradation.
- Investigate the relationship between ballast moisture and fouling assessment capabilities of the dielectric dispersion analysis method used by System 3.
- Install both GPR systems on the FRA T18 track inspection vehicle and compare the results with those from the standard hi-rail platform.

Two revenue service sites were established: (1) a high tonnage/heavy-axle load UP western site for ballast degradation monitoring by System 1 and (2) a mixed traffic/low tonnage Amtrak eastern site for monitoring moisture changes under static fouling condition by System 3. Three GPR surveys were performed at both sites.

Although there are significant differences between them, based on the evaluations performed the two systems involved in Phase 2 represent the current state-of-the-art for GPR track assessment technology. The evaluation results are summarized in the following subsections.

6.1 Western Site

The following is a summary of the findings of the System 1 evaluation at the western site:

- Fouling results from the three surveys suggested a slight increase in the level of fouling in six of the ballast boxes in the curve zone over the 10-month period of testing with most of the increase occurring between the October 2012 and March 2013 surveys.
- No measurable change in fouling was observed in boxes 1 and 3 in the curve zone.
- Results from the ballast box test in the tangent zone showed no measurable change in fouling over the 10-month period, except for in boxes 1 and 2, where a nominal increase in fouling was noted between May 2012 and October 2013.
- Results obtained over the MP 49 to 51 track segment showed no significant change in ballast fouling. The modeled FI over 2 miles varied from clean to moderately clean. An increase in the FI west of approximately MP 50.55 was attributed to the westerly limit of ballast undercutting undertaken in 2011.

Results from the western site indicated that scattering analysis of the 2-GHz GPR signal is capable of providing a repeatable, stable method of determining the level of ballast fouling which can be used to monitor the change in fouling over time. Measurable change in the FI (i.e., a change within the limits of detectability) is currently defined by System 1 as a variation in +/- .2 BFI.

6.2 Eastern Site

The following is a summary of the findings of the System 3 evaluation at the eastern site:

- GPR surveys of the eastern site by System 3 were able to discern changes in the moisture within the ballast and subballast layers, as well as at the ballast, sub-ballast, and subgrade interfaces that correlated well with localized rainfall events recorded by NOAA.
- Moisture profiles were calculated by System 3 using a recently developed frequency-relation analysis tool that is based on comparisons of different frequency bands in the returning GPR signal.
- Increased moisture had a slight influence on the ballast fouling interpretation when the ballast depth was calculated using a constant time window. The fouling results improved when the time window was adjusted by changing the assumed dielectric constant of the wet ballast.

Results of the eastern site evaluation confirmed the influence of moisture on the interpretation of ballast layer depth and fouling using the dielectric dispersion technique. Increasing moisture creates a higher dielectric value of the layer material, which slows the GPR signal. Layer depth is calculated from the measured return time of the signal and the assumed dielectric value of the material. Therefore, changes in moisture influence the layer depth calculation, which, in turn, influences the fouling analysis. Development of the frequency-relation analysis tool for moisture profile interpretation by System 3 should enhance the ability to adjust the dielectric value in the fouling window analysis.

6.3 T18 Evaluation

GPR systems 1 and 3 were both successfully installed on the T18 vehicle and produced outputs that were comparable to the outputs from their hi-rail platforms. The following are specific observations, as provided by both systems:

- System 3:
  - Installations of the GPR system took less than 1 hour.
  - Deployment of the T18 GRMS axle did not alter the GPR data, despite a 2-inch difference in antenna height.
  - There was some “ringing” of the GPR signal due to reflections from metal under the T18 platform, most notably from the steel plow located near the wheels of the car. Echo-absorbing foam insulation was effective in reducing the ringing.
  - GPR data was collected on distance-based encoder input using one of the T18 onboard encoders, which provided a suitable signal for triggering the GPR. The geometry data from the T18 was based on a separate encoder.
  - The GPR data was aligned to the track geometry and GRMS data simply by matching the signal to track feature locations and by stretching or shrinking the GPR data, as needed, to match other data sets. Future integration of GPR and other data from the T18 can be effectively done by periodically tagging the GPR file with markers from the sync-count file.
  - Once the GPR data and track geometry/GRMS data were aligned, the GPR data was resampled to 1-foot increments to match the geometry/GRMS increment.

- System 1
  - GPR system was successfully integrated with the T18 existing location, track geometry, and GRMS systems.
  - T18 platform allows use of antenna shields that are too heavy for use on the hi-rail platform.
  - Location of center 2-GHz antenna may be possible on the T18 vehicle. Location of shoulder and center 2-GHz and 400-MHz antennas should be possible on the T16 vehicle.

In addition, truck-mounted antennas work much better than pilot or vehicle body mounting. Truck-mounted antennas reduce clearance issues and interference from running rails on curves. There do not appear to be significant limitations to data collection speeds for GPR technology. Modern data acquisition equipment has sufficient collection bandwidths to accommodate high speed GPR inspections.

7. Conclusion

The development of GPR as a track substructure assessment tool has benefitted over the past 10 years from research sponsored by FRA, AAR, universities, and the internal research efforts of GPR providers. At present, GPR has the capability and is being used by some North American railroads to characterize ballast conditions over hundreds of track miles annually for maintenance planning purposes. GPR is also being used to address localized substructure issues, such as subgrade deformation and drainage problems, as well as for maintenance planning and prioritization. In either case, GPR has the capability to nondestructively visualize otherwise invisible track substructure conditions.

However, there are some basic key areas in which GPR can benefit from continued research and improvement; for example, in the assessment of the substructure below the primary ballast layer, and in real-time data processing and analysis. Both items are recognized as difficult challenges for GPR and represent long-term research goals. The rationale for these research paths are as follows:

- Track substructure conditions below the ballast that can greatly affect track performance, such as subgrade soil type, strength, moisture content, and subsurface water infiltration, are often unknown or misunderstood. Current investigative methods, including cross trenching, boring, or penetrometer testing, are destructive, slow, and/or conducive only to spot testing. Development of GPR to interpret and characterize subgrade soil properties and moisture conditions would greatly enhance track geotechnical capabilities. Correlation with other track structural parameters and condition indicators will provide the data needed to assess the range of properties to be expected for various track types and conditions.
- The T18 track inspection vehicle was shown to be a viable platform for current GPR technologies in Phase 2. Adding GPR substructure data to the track geometry and other track performance data sets significantly enhances the capability of track inspection vehicles. GPR data, however, is currently not available as a real-time output display, as are other T-18 track measurement systems. Automation of GPR signal processing and analysis, working toward real-time or near real-time data output, is a long-term research goal for GPR application.

8. References

1. Read, David, et al. (September 2017). "Ground Penetrating Radar Technology Evaluation on the High Tonnage Loop: Phase 1." DOT/FRA/ORD-17/18. Federal Railroad Administration. Washington, DC. Available at: https://www.fra.dot.gov/eLib/Details/L19031.
2. Selig, E. and J. Waters. (1994). *Track Geotechnology and Substructure Management*, Thomas Telford Publications. London, UK.

Abbreviations and Acronyms

AAR	Association of American Railroads
BFI	Ballast Fouling Index
FI	Fouling Index
FRA	Federal Railroad Administration
GPR	Ground Penetrating Radar
GRMS	Gage Restraint Measuring System
HTL	High Tonnage Loop
NOAA	National Oceanic and Atmospheric Administration
TTC	Transportation Technology Center
TTCI	Transportation Technology Center, Inc.
UP	Union Pacific Railroad